

Nucleation and growth of Ag films on a quasicrystalline AlPdMn surface

V. Fournée,* T. C. Cai,† A. R. Ross, T. A. Lograsso, J. W. Evans, and P. A. Thiel‡

Departments of Chemistry, Materials Science and Engineering, and Mathematics, and Ames Laboratory, Iowa State University, Ames, Iowa 50011

(Received 23 October 2002; published 21 January 2003)

Nucleation and growth of thin films of Ag on the fivefold surface of an $\text{Al}_{72}\text{Pd}_{19.5}\text{Mn}_{8.5}$ icosahedral quasicrystal is studied with scanning-tunneling microscopy. For low coverages, flux-independent island nucleation is observed involving adatom capture at “traps.” With increasing coverage, islands start growing vertically, but then spread, and ultimately form hexagonal nanocrystals. These have fcc symmetry and pyramidlike multilayer stacking along the $\langle 111 \rangle$ direction. The constituent hexagonal islands have five different orientations, rotated by $2\pi/5$, thus reflecting the symmetry of the substrate.

DOI: 10.1103/PhysRevB.67.033406

PACS number(s): 61.44.Br, 68.55.Ac

There is currently a broad interest in heteroepitaxial growth, motivated by the possibility of fabricating nanostructures on solid surfaces for technological applications. In particular, growth modes are being considered as an alternative to optical lithography to obtain self-organized patterns of nanosized features. Here we explore a class of heteroepitaxial systems in which a metallic thin film is deposited on a structurally complex substrate: the surface of a quasicrystal. Quasicrystals are complex alloys with long-range, atomic-scale order, but without periodicity.¹ Their bulk structure is most commonly found to be icosahedral, thus possessing elements of fivefold rotational symmetry. Their free surfaces appear to be flat truncations of the bulk structure, or very nearly so, and are therefore intrinsically complex. We will present here an analysis of the nucleation and growth mechanisms operating in this system. This is helpful to understand under what conditions a quasicrystalline surface can be used as a substrate for growing “artificial quasicrystals.”^{2,3} By “artificial quasicrystal,” we mean a thin film that would be constrained sufficiently by the potential-energy surface of the substrate to adopt a nonperiodic structure and the forbidden rotational symmetry characteristic of the quasicrystal, even though the film material normally would form a periodic lattice. So far, quasicrystals can only be formed from the combination of at least two elements and it would be very informative, in itself, if a quasiperiodic film were realized, as quasiperiodicity could be considered independently from chemical composition effects. Even if pseudomorphic growth does not occur, there is also interest in whether and how the unusual symmetry of the substrate is transferred to the film.

However, the structure of a thin film cannot be considered separately from the mechanism and kinetics of its formation, since the final structure is often the result of specific growth conditions.⁴ Conversely, there exists a possibility that if growth of thin films on quasicrystals is understood, then growth conditions might be tailored to favor formation of artificial quasicrystals. This motivates our description, in this paper, of the growth of a Ag thin film on the archetypical fivefold surface of the icosahedral AlPdMn quasicrystal. Using scanning-tunneling microscopy (STM), we elucidate the nucleation mechanism, the growth mode, and the transition to a bulklike structure in the film. We also clarify the way in

which the unique rotational symmetry of the substrate affects the final structure of the film, and comment upon future strategies most likely to yield artificial quasicrystals.

In our experiments, Ag atoms are produced by evaporation of the pure metal and impinge individually at a given flux F on the surface, where they diffuse and nucleate a film. (The sticking coefficient is safely assumed to be unity, and evaporation of Ag from the surface is entirely negligible.) Different morphologies can result, of which the most “desirable” is smooth layer-by-layer growth, since this maximizes the film-substrate interaction and hence maximizes the probability of pseudomorphism (adoption of the substrate structure by the film). Macroscopically, and under conditions where thermodynamic equilibrium is reached, smooth layer growth is favored if the film has relatively low surface energy, i.e., if $\gamma_{\text{Ag}} < \gamma_{\text{QC}} - \gamma^*$.⁵ Here, γ_{Ag} and γ_{QC} are the surface free energies of the film and substrate, respectively, and γ^* is the interfacial energy. Based on contact angle measurements of liquid droplets in air, γ_{QC} should be low, although its absolute value has not been estimated.⁶ The value of γ_{Ag} (1.172 J/m^2) is also low and very similar to γ_{Al} (1.199 J/m^2),⁷ Al being the major constituent of the topmost atomic layer of the i -AlPdMn surface.⁸ Considering these facts, and ignoring (until later) the contribution of γ^* , the choice of Ag as a film could, indeed, lead to smooth growth. Ag is also immiscible with Al in the bulk and the heat of mixing of the two metals is negative (-0.61 eV), hence giving a low probability of surface alloy formation.

We performed our experiments on a quasicrystal sample extracted from a single grain with composition $\text{Al}_{72}\text{Pd}_{19.5}\text{Mn}_{8.5}$ grown by the Bridgman method. It was cut perpendicular to a fivefold-symmetry axis and mechanically polished down to a final roughness of $0.25 \mu\text{m}$. A clean surface is obtained after repeated cycles of Ar^+ sputtering and annealing up to 900 K in an ultrahigh vacuum chamber, which is equipped with an Omicron scanning-tunneling microscopy.

This method of surface preparation leads to a terrace and step morphology.⁹ The average size of the terraces is quite large, and it is possible to scan the W tip over an area that is several hundreds of nanometers on a side and with a corrugation of about 0.8 \AA . Both the step heights measured (2.4 , 4.1 , and 6.5 \AA) and the fine structure observed on the terraces

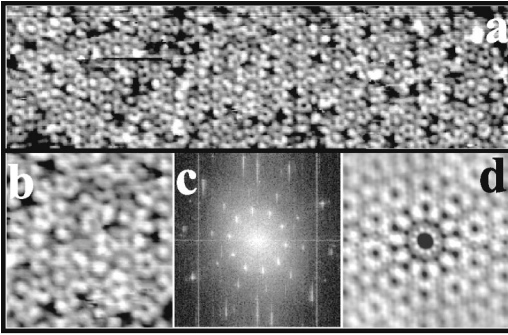


FIG. 1. STM images (a) $30 \times 8 \text{ nm}^2$ and (b) $6 \times 6 \text{ nm}^2$ of the fine structure on a flat terrace of the fivefold surface of the $i\text{-Al}_{72}\text{Pd}_{19.5}\text{Mn}_{8.5}$ quasicrystal. (c) is the fast-Fourier transform (FFT) and (d) the autocorrelation function of the STM image revealing the long-range order and a tenfold symmetry compatible with the fivefold symmetry of the surface.

(Fig. 1) are fully consistent with a laterally bulk-terminated surface, consisting of atomic “planes” that are cross sections of the bulk structure.¹⁰ The surface actually consists of two planes separated by only 0.4 \AA , of which the top plane probed by the scanning-tunneling microscopy is mainly Al and the second is about $\text{Al}_{50}\text{Pd}_{50}$.⁸ The fine structure revealed by high-resolution images varies from terrace to terrace. The fast-Fourier transform, and the autocorrelation function, of each terrace shows, however, the same tenfold symmetry, consistent with the fivefold symmetry of the surface. We do not describe further its characteristics and instead focus on the nucleation and growth of the metallic film on this high-quality quasiperiodic substrate.

The data resolve three different regimes in film thickness or coverage (expressed in units of monolayers, ML). We first describe the regime where the coverage of the film is much less than that would be required to fill a single layer, i.e., below 1 ML. STM images of the surface exposed to 0.2 ML of Ag deposited with a flux $F = 10^{-3} \text{ ML/s}$ show the formation of islands that are one atom high (2 \AA) above the surface. Due to the roughness of the substrate, STM cannot reveal the internal structure of the islands. The top panel of Fig. 2 shows that the average island density, N_{av} (in nm^{-2}) at 0.2 ML, does not vary significantly with flux. The bottom panel shows the normalized island size distribution f for a single flux ($F = 10^{-3} \text{ ML/s}$). The statistics in the data of Fig. 2 are extremely good, since the data are deduced from STM images of many terraces, spanning an area equal to $2 \times 10^5 \text{ nm}^2$, and thousands of islands.

The flux scaling of N_{av} ,¹¹ as well as the shape of f ,^{12,13} provide insight into the nucleation process underlying island formation. Classic analysis for deposition on perfect crystalline surfaces shows that if (homogeneous) nucleation of stable islands requires aggregation of $i+1 \geq 2$ diffusing adatoms, then one has $N_{\text{av}} \sim F^{i/(i+2)}$.^{11–13} (The dashed line at the top of Fig. 2, for instance, shows the scaling relationship expected for $i=1$.) N_{av} is seen to be independent of F . This rules out the possibility of homogeneous nucleation with critical size $i \geq 1$ on the quasicrystal surface but indicates one of two alternative scenarios. The first is heterogeneous nucle-

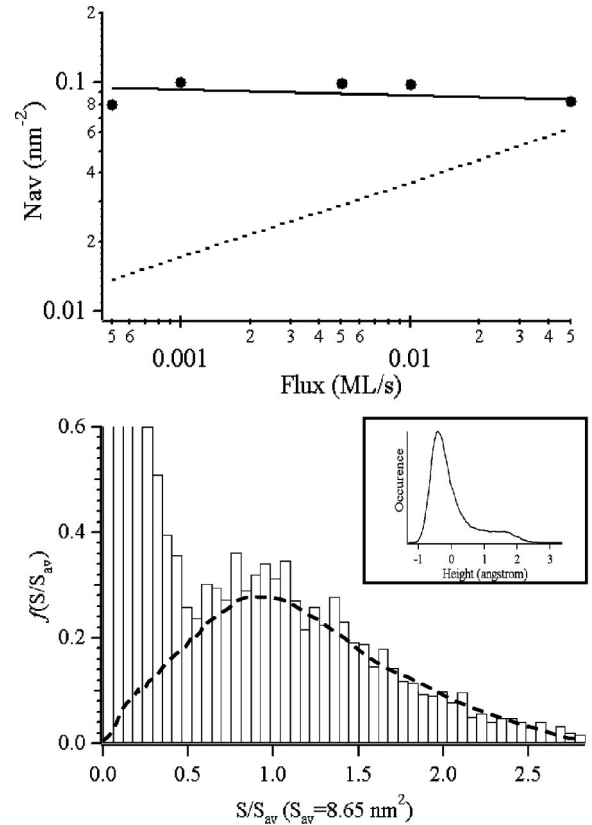


FIG. 2. Top panel: average island density N_{av} versus flux, for $\theta=0.2 \text{ ML}$. The dashed line shows the scaling behavior expected for $i=1$. Bottom panel: normalized island size distribution $f(S/S_{\text{av}})$ from STM images for Ag/AlPdMn at 0.2 ML and $F=10^{-3} \text{ ML/s}$. The island size distribution is defined by $N_S/N_{\text{av}} \approx S_{\text{av}}^{-1} f(S/S_{\text{av}})$, where N_S is the density of islands of size S , and S_{av} is the average island size. The dashed line show the “true” shape of f . The inset is the height histogram of a terrace ($150 \times 150 \text{ nm}^2$) covered by 0.2 ML of Ag, demonstrating its continuous nature.

ation by irreversible capture of diffusing adatoms at specific quasilattice trap sites. The second (denoted by $i=0$) is homogeneous nucleation by random irreversible place exchange of an adatom with the substrate, thereby forming a stable nucleus for island growth.¹³

The shape of the island size distribution can be used to decide between these two scenarios. Figure 2 shows that f has a local maximum at the average size S_{av} , as expected for heterogeneous nucleation¹⁴ but not for homogeneous nucleation with $i=0$.¹³ (The apparent large population of small islands in Fig. 2 is an artifact resulting from the intrinsic corrugation of the substrate, and the consequent inability to choose a height cutoff that distinguishes cleanly between the substrate and the islands.) The fact that N_{av} is independent of F , together with the observed shape of f , unambiguously points to heterogeneous nucleation at specific sites.

The second coverage regime extends from 1 to 10 ML, in which much rougher films are observed. At a coverage of only 1 ML, height histograms reveal islands which are up to five atoms high. Ag islands appear as “needles” covering the surface in three-dimensional (3D) plots of the STM images [Fig. 3(a)]. The formation of these “needles” implies an easy

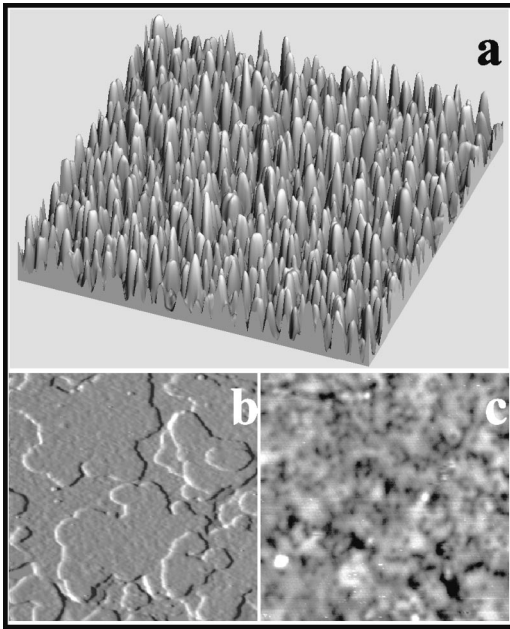


FIG. 3. (a) 3D view of an STM image ($200 \times 200 \text{ nm}^2$) of Ag/AlPdMn. (1 ML, $F = 10^{-3} \text{ ML/s}$). STM image (b) 100×100 and (c) $27.6 \times 27.6 \text{ nm}^2$ of Ag/AlPdMn at 5 ML and $F = 3 \cdot 10^{-3} \text{ ML/s}$.

uphill motion of Ag atoms, i.e., it implies that roughness is not a result of kinetic limitations.

The effect of the quasicrystalline substrate on Ag film roughness is made apparent by comparing the growth on a substrate that is similar in chemical composition but different in its atomic structure:⁸ Al(111). STM images of an Al(111) surface covered by 0.2 ML of Ag deposited under the same conditions as for the quasicrystal reveal a completely different morphology. Here the growth is pseudomorphic, with formation of triangular-shaped islands and an island density that depends on the flux, in clear contrast to the quasicrystal substrate.

As coverage increases further in the second regime, from 1 to 10 ML, the roughness of the film does not vary (from $\approx 1 \text{ nm}$) but the needles grow laterally, up to 30 or 40 nm. Islands have a rather lumpy aspect at 1.7 ML and evolve toward flat-topped structures as the lateral growth proceeds, as shown in Fig. 3(b) at 5 ML. An enlargement of one of these flat islands [Fig. 3(c)] reveals a complex structure with zones of bright contrast forming a disordered network. The associated roughness is of the same order of magnitude as for the clean substrate (about 0.8 \AA , peak to peak). These rela-

tively flat-topped islands form the bases for the features that develop next.

The third growth regime is above 10 ML, where the film features again grow vertically (roughness increases from about 1 to 5 nm at 100 ML), forming pyramidlike nanocrystals with flat hexagonal tops, as shown in Fig. 4(a). The set of spikes separated by about 2.3 \AA in the height histogram [Fig. 4(b)] confirms the formation of atomically flat layers with a uniform vertical stacking. Here, the film structure is remarkably similar to that of Ag on Ag(111),¹⁶ suggesting that growth is controlled by the same kinetic factors as in homoepitaxy. (Specifically, the key kinetic limitation is inhibited interlayer transport due to a so-called step-edge barrier). The convergence to homoepitaxy in this regime is supported by atomically resolved STM images of the nanocrystal tops, one of which is shown in Fig. 4(c). The hexagonal lattice of Ag(111) is clearly observed, confirming that the film has adopted the bulk Ag structure. However, even a film as thick as 100 ML *still reflects* the symmetry of the substrate, because the edges of the hexagonal islands display specific relative orientations. The angle between edges of pairs of islands always equals a multiple of 12° (0, 12, 24, 36, etc.), i.e., a multiple of $(2\pi/5 - 2\pi/6)$. In other words, the fcc Ag islands display a fivefold-symmetrical arrangement. Note that the STM data indicate the threefold axis of crystalline Ag parallels the fivefold axis of the substrate.

Our work has several major implications, both for the general understanding of epitaxy on complex substrates, and for developing strategies toward pseudomorphic film growth. First, nucleation is heterogeneous, not homogeneous, which means that island nucleation does not take place randomly, but at specific sites. While this is a disadvantage in obtaining smooth layer growth (it effectively removes flux as an experimental variable), it could potentially be turned to advantage in developing strategies for fabricating organized patterns of nanostructures on a surface.

Second, the Ag film does *not* grow smoothly and this reflects thermodynamic factors up to 10 ML, but kinetic factors for thicker films. Returning to the balance of free-energy terms that determines film morphology, the extreme roughness at low coverage on the quasicrystal could mean either that γ_{QC} is lower than γ_{Ag} , the interfacial energy γ^* is prohibitively high, or that there exists a combination of these effects. Smooth growth on the Al(111) substrate together with the top layer of the quasicrystal being almost pure Al suggest that γ_{Ag} and γ_{QC} should not be significantly different

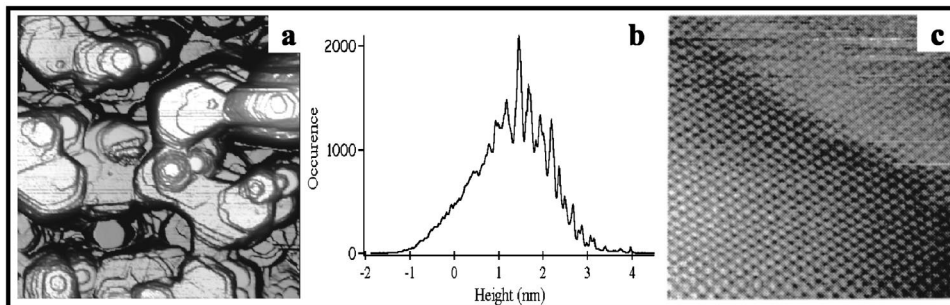


FIG. 4. (a) STM image ($200 \times 200 \text{ nm}^2$) of Ag/AlPdMn at 100 ML and $F = 2 \cdot 10^{-2} \text{ ML/s}$. (b) Height histogram from a terrace ($300 \times 300 \text{ nm}^2$) covered with 10 ML of Ag/AlPdMn deposited at flux $F = 10^{-2} \text{ ML/s}$. (c) Atomically resolved STM image ($10.8 \times 10.8 \text{ nm}^2$) on top of the hexagonal islands at 100 ML and $F = 2 \cdot 10^{-2} \text{ ML/s}$.

and this leads us to postulate that the interfacial energy must be important to explain the rough growth. A high value of γ^* is a reasonable possibility, since the nonperiodic arrangement and fivefold symmetry of the substrate could well introduce high strain into the film resulting from the interfacial mismatch (dimensional and orientational). Furthermore, we have observed similar roughness at low coverages in a similar system—Al on a fivefold surface of icosahedral AlCuFe (Ref. 15)—which also points to a significant effect of γ^* .

The third main implication from this work is that, even though the Ag film cannot adopt fivefold symmetry on an atomic scale, it can do so on a mesoscopic scale. Here, we are referring to the fivefold orientations of the hexagonal nanocrystals in the third coverage regime, above 10 ML. The Ag(111) nanocrystals with orientation determined by the substrate are formed below 10 ML and, once these are formed, one essentially has simple Ag(111) homoepitaxy, which propagates this orientation into thicker films, leading to fivefold twinning. Twinning in thick crystalline films or overlayers on top of quasicrystals appears to be quite general, based on the fact that it has been observed also in several different, but analogous, systems: PtAl (Ref. 3) and AuAl overlayers² on the tenfold surface of a decagonal quasicrystal, and Al films¹⁷ and cubic alloy overlayers¹⁸ on the same fivefold surface studied here.

As a final remark, we have observed that a surfactant, oxygen, can smoothen a thick (100-ML) Ag film on the quasicrystal substrate, but the resultant film still displays a nano-

structured pattern, in the shape of an array of fivefold twins of fcc Ag separated by grain boundaries. Such patterns cannot be created by deposition of Ag on Ag(111). These observations also confirm that the pyramidal morphology and large roughness of the films above 10 ML is kinetically limited, but that lateral twinning is not.

This leads us to conclude that the best approach to obtain a smooth, pseudomorphic film on a quasicrystalline surface may be to go to lower temperatures, where kinetics will promote homogeneous nucleation and suppress upward migration. Further, coverages below 10 ML are most promising, since here the substrate clearly exerts a strong influence on the structure of the film.

In more general terms, Ag film growth on this fivefold quasicrystal exhibits several phenomena (heterogeneous nucleation, rough growth at low coverages, twinning at high coverages) whose relationship to the unique atomic structure of the substrate presents interesting dimensions in the understanding of epitaxy.

We would also like to note that we recently became aware of a publication by Franke *et al.* describing the successful growth of epitaxial Sb and Bi films on quasicrystalline surfaces.¹⁹

This work was supported by NSF Grant No. CHE-0078596, and performed at Ames Laboratory (which is operated for the US DOE by ISU under Contract No. W-7405-Eng-82).

*Present address: LSG2M, CNRS-UMR 7584, Ecole des Mines, F-54042 Nancy, France.

†Present address: Brookhaven National Laboratory, P.O. Box 5000, Upton, NY 11973-5000.

‡Corresponding author. Email address: thiel@ameslab.gov

¹D. Shechtman *et al.*, Phys. Rev. Lett. **53**, 1951 (1984).

²M. Shimoda *et al.*, Surf. Sci. **482–485**, 784 (2001).

³M. Shimoda *et al.*, Surf. Sci. **507**, 276 (2002).

⁴P. A. Thiel and J. W. Evans, J. Phys. Chem. B **104**, 1663 (2000).

⁵E. Bauer and J. H. van der Merwe, Phys. Rev. B **33**, 3657 (1986).

⁶J. M. Dubois *et al.*, in *Proceedings of the Sixth International Conference on Quasicrystals (ICQ6)*, edited by S. Takeuchi and T. Fujiwara (World Scientific, Singapore, 1998), pp. 733–740.

⁷L. Vitos *et al.*, Surf. Sci. **411**, 186 (1998).

⁸M. Gierer *et al.*, Phys. Rev. Lett. **78**, 467 (1997); M. Gierer *et al.*, Phys. Rev. B **57**, 7628 (1998); M. J. Capitan *et al.*, Surf. Sci. **423**, L251 (1999); R. Bastasz *et al.*, in *MRS Conference Proceedings: Quasicrystals*, edited by E. Belin-Ferré, P. A. Thiel, K. Urban, and A.-P. Tsai, Mater. Res. Soc. Symp. Proc. No. **643** (Materials Research Society, Pittsburgh, 2001), p. K11.1.1.

⁹P. A. Thiel *et al.*, in *Physical Properties of Quasicrystals*, edited by Z. Stadnik (Springer-Verlag, Berlin, 1998), pp. 327–359.

¹⁰L. Barbier *et al.*, Phys. Rev. Lett. **88**, 085506 (2002); J. Ledieu *et al.*, Surf. Sci. Lett. **492**, L729 (2001).

¹¹J. A. Venables, Physica A **239**, 35 (1997).

¹²M. C. Bartelt and J. W. Evans, Phys. Rev. B **54**, R17 359 (1996).

¹³D. D. Chambliss and K. E. Johnson, Phys. Rev. B **50**, 5012 (1994).

¹⁴For each trap, one expects a Poisson distribution of island sizes, with mean size controlled by the area of the associated capture zone. We determine the full size distribution by averaging these Poisson distributions over the (monomodal) distribution of capture zone areas, as determined from STM images. See also P. A. Mulherin and J. A. Blackman, Philos. Mag. Lett. **72**, 55 (1995).

¹⁵T. Cai *et al.*, Surf. Sci. (to be published).

¹⁶J. Vrijmoeth *et al.*, Phys. Rev. Lett. **72**, 3843 (1994); W. C. Elliot *et al.*, Phys. Rev. B **54**, 17 938 (1996).

¹⁷B. Bolliger *et al.*, Phys. Rev. B **63**, 052203 (2001).

¹⁸Z. Shen *et al.*, Phys. Rev. B **58**, 9961 (1998).

¹⁹K. J. Franke *et al.*, Phys. Rev. Lett. **89**, 156104 (2002).